

# Evaluation of the MgO Protective Layer Deposited by Oxygen Ion-Beam-Assisted-Deposition Method in ac PDPs

Zhao Hui Li, Eou Sik Cho, Seong Jae Hong, and Sang Jik Kwon\*

Department of Electronics Engineering, Kyungwon University, San 65, Bokjung-dong, Soojung-gu, Seongnam City, Kyunggi-do 461-701, Korea

TEL:82-31-750-8517, e-mail: sjkwon@kyungwon.ac.kr

Keywords : IBAD, MgO, PDP

## Abstract

MgO thin films were deposited by  $O^+$  IBAD method and results showed assisting oxygen ion beam energy plays a significant role in characteristics of MgO thin films. The lowest firing inception voltage, the highest brightness and the highest luminous efficiency were obtained when oxygen ion beam energy was 300 eV.

## 1. Introduction

Plasma display panels (PDPs) are expected to be one of the most promising candidates for the large-sized high definition televisions (HDTV), due to the advantages of occupying a small space, a wide viewing angle, and a low weight. In ac-PDPs, MgO thin film has been widely used as a surface protective layer for dielectric materials because of its low sputtering yield, very large band gap and large secondary electron emission coefficient (SEEC)  $\gamma$ . So the MgO layer plays an important role in keeping the breakdown voltage low and in limiting the damages due to energetic ions. The MgO layer is important both for the efficiency and for lifetime.

The MgO thin film is currently prepared by electron beam (e-beam) evaporation method and ion plating.[1] But some problems are shown in the MgO deposited with the e-beam evaporation: cracks during the annealing process and high erosion as a consequence of ion bombardment in the glow discharge.[2~4] The IBAD method is one of the methods to resolve these problems.

During deposition, the MgO is decomposed into Mg and O atoms at the first stage of the vacuum evaporation, and the decomposed Mg and O atoms arrive at the substrate as building up one by one and finally are re-crystallized as MgO. Thus the oxygen feeding during MgO evaporation is effective for improving quality of the stoichiometrical quality of

MgO thin film. Some papers reported that oxygen feeding method during MgO deposition improved the characteristics of MgO for AC PDPs. Other papers reported that the ion beam assisted method was appropriate to deposit MgO for a protective layer for AC PDPs.[5~9]

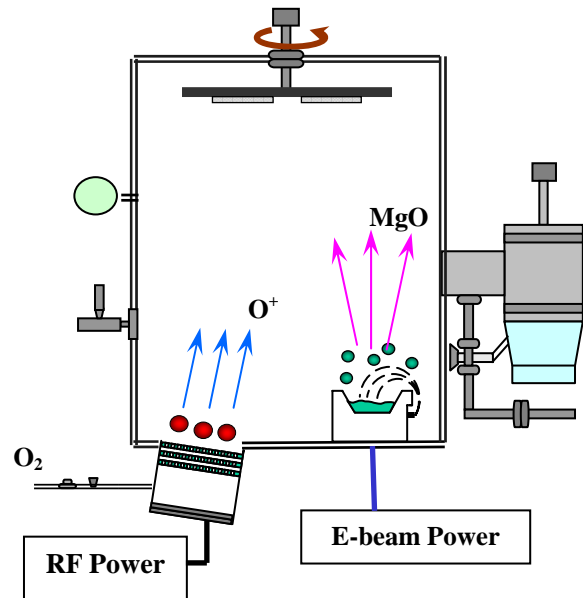


Fig. 1. Schematic of IBAD system.

So, in this paper we had studied the structural and discharging characteristics of the MgO thin film, which prepared by oxygen ion beam assisted deposition method in order to improve the characteristics of AC PDPs.

## 2. Experimental

The 2-inch samples were prepared with glass substrate (PD-200, ASAHI) in this experiment. The thickness of address electrode was about 8  $\mu\text{m}$  and

width was about 200  $\mu\text{m}$ . The thickness of dielectric layer was approximately 24  $\mu\text{m}$ , and the barrier rib had a height of about 130  $\mu\text{m}$ . The green phosphor is only coated using the screen-printer and the thickness is about 10  $\mu\text{m}$ . The width of the bus electrodes was approximately 80  $\mu\text{m}$  and the height was about 8  $\mu\text{m}$ . The panels were set in the chamber and were driven by the square pulse, which width was 3  $\mu\text{s}$  and frequency was 50 kHz. The discharging gas is the Ne + Xe (4%) mixture gas and the operation pressure is 400 Torr. Before discharging test, the annealing process was done at 300 °C for 1 hour. The MgO thin film was deposited by the IBAD method. Figure 1 shows the schematics of the IBAD system. The e-beam is used to evaporate MgO (99.99%). The oxygen (99.99%) flow rate was 10 sccm. The Oxygen ion was produced by the RF ion source and carried out by the ion gun. The power of the ion was fixed at 200 W. The base pressure was  $3 \times 10^{-6}$  Torr and the working pressure was  $1.6 \times 10^{-4}$  Torr. The temperature was fixed at 300 °C. The assisting oxygen ion beam energy was varied from 100 eV to 500 eV. The deposition rate was 5 Å/sec, and the deposition thickness was about 5,000 Å.

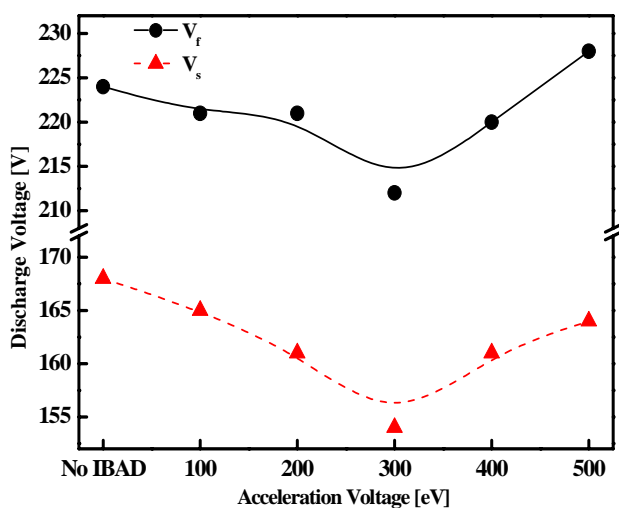


Fig. 2. Firing voltage and sustain voltage versus acceleration voltages.

The firing voltage ( $V_f$ ), the sustaining voltage ( $V_s$ ) and the discharging current were measured with current probe (Tektronix, TCPA300) and oscilloscope (TDS-540C). The brightness was measured with the chroma meter (CS-100A). The crystal orientation of the MgO thin film was investigated using the X-ray Diffraction (XRD, Rigaku). And the surface feature is

measured with the atomic force microscope (AFM).

### 3. Results and discussion

The  $V_f$  and  $V_s$  were measured and the secondary electron emission coefficient  $\gamma$  for  $\text{Ne}^+$  is calculated according to the well-known Paschen law

$$V_f = \frac{Bpd}{\ln[Apd/\ln(1+1/\gamma)]} \quad (1)$$

where, A, B are constants, and p is the gas pressure and d is the distance of electrode,  $\gamma$  is the secondary electron emission coefficient. From the above Eq. (1), we can see that the  $\gamma$  value decreases with the  $V_f$  increasing. Figure 2 shows that the minimum  $V_f$  and the largest  $\gamma$  are obtained at 300 eV. The  $V_f$  decreases with the assisting ion beam energy from the No IBAD to 300 eV, but the  $V_f$  increases when the assisting ion beam energy is over 400 eV.

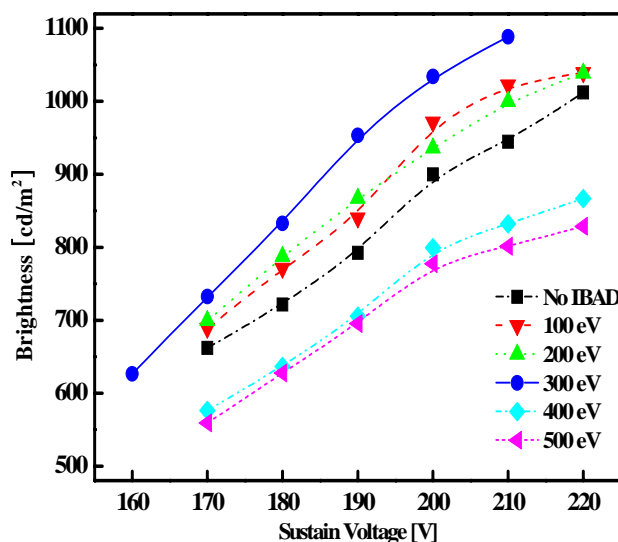
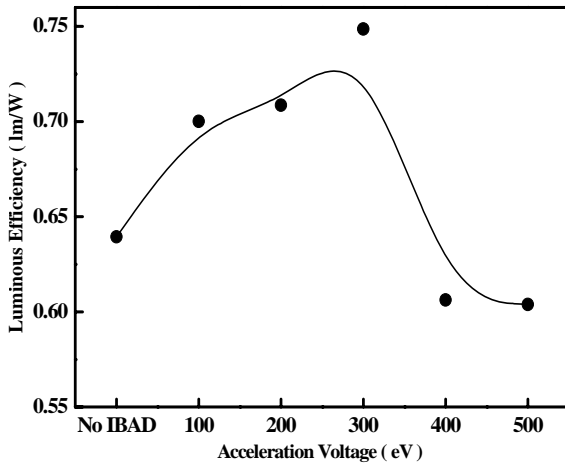


Fig. 3. Brightness of each sample deposited with varied acceleration voltages.

To improve the brightness is one of key issues for AC PDPs. We measured the brightness of each sample from  $V_s$  to  $V_f$  at the step of 10 V. See Fig. 3. It is clear that the brightness of the samples deposited with assisting ion energy of 300 eV is higher than the others at each sustaining voltage. The brightness increases as the assisting ion beam energy from No IBAD to 300 eV. However, the brightness decreases as the assisting ion beam energy increased above 400 eV.



**Fig. 4. Luminous efficiency versus acceleration voltages.**

Luminous efficiency is also one of the main issues of the PDP industry. Luminous efficiency is must be improved to lower the electronic drivers cost. In this paper, we measured the brightness, the discharging current and the applied voltage. The luminous efficiency is calculated and shown in the Fig. 4 as the function of the assisting ion beam energy. The luminous efficiency is increasing with the assisting ion beam energy increasing form 100 eV to 300 eV, which is higher than the No IBAD. But compared to No IBAD, the brightness is much lower when the assisting ion beam energy is over 400 eV. The highest luminous efficiency is obtained when the assisting ion beam energy is 300 eV.

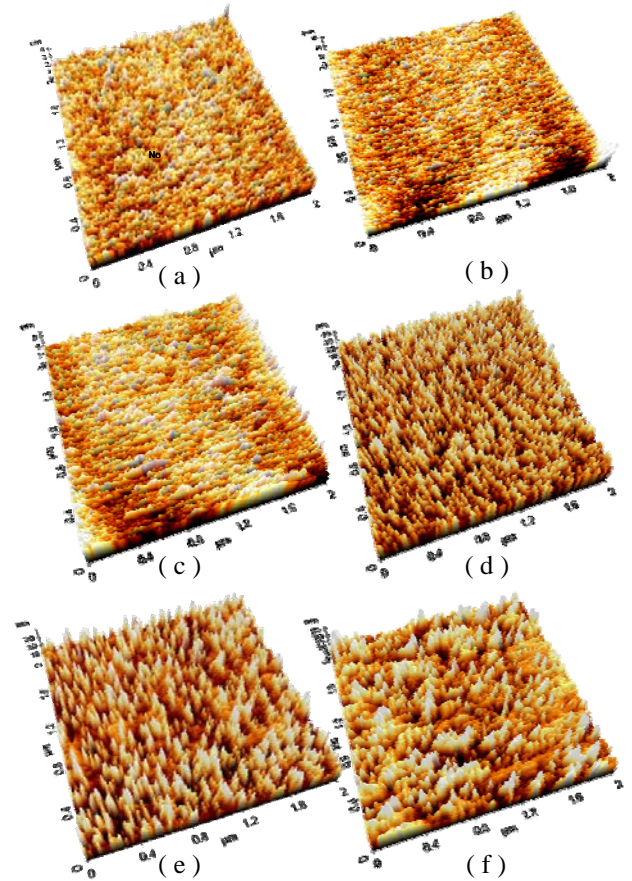


**Fig. 6. AFM images of MgO versus acceleration voltages (a) No IBAD, (b) 100 eV, (c) 200 eV, (d) 300 eV, (e) 400 eV, and (f) 500 eV.**

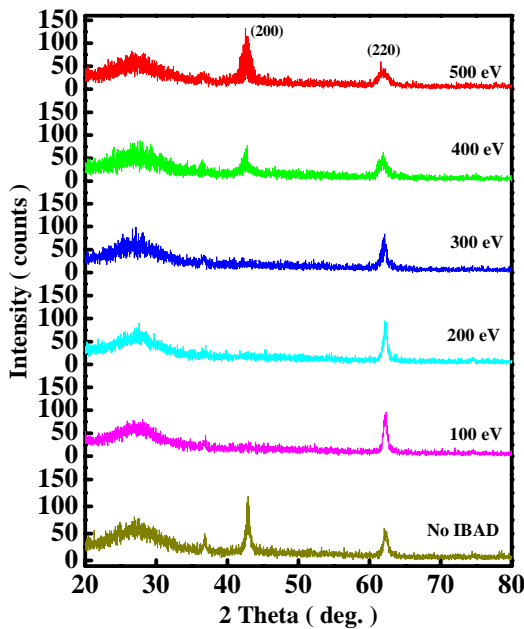


**Fig. 5. XRD spectra of MgO thin films.**

The crystalline of MgO has important effect on the discharge characteristics, and increases in the diffracted (111) peak intensity of MgO thin film results in the decrease in firing voltage. The secondary electron emission coefficient for (111) orientated MgO thin film is substantially larger than other directions. Figure 5 shows the XRD spectra of the annealed MgO film. The No IBAD sample has (111), (200) and (220) preferred orientation. The MgO prepared with IBAD has weak peak (111). In our experiment the weak peak (111) may be produced by the ion bombardment during deposition. The (200) peak is appeared at the assisting ion beam energy above 400 eV, and the (200) peak intensity increases with assisting ion beam energy increasing. On the other hand, the (220) peak intensity decreases with assisting ion beam energy increasing. It may be the preferred orientation transition from (220) to (200) in order to produce a stable orientation as a result of increase of kinetic energy of the oxygen ion. Therefore, we can say that the assisting ion beam energy plays an important role

in effecting the preferred orientation and the intensity of the peaks.

Figure 6 shows AFM images of the MgO thin film. The fine needle-shaped grain growth occurs on the surface of the substrate, which was prepared with assisting ion beam energy of 300 eV, as shown in Fig. 6(d). However, with the increase of assisting ion beam energy, the mountain-shaped crystallite structure comes out as shown in the Fig. 6(e), (f) as a result of aggregation of gains. The surface RMS roughness is 0.420 nm, 0.357 nm, 0.618 nm, 4.386 nm, 3.761 nm, 2.320 nm for substrates, which deposited at No IBAD~500 eV, respectively. The largest surface RMS roughness ( $R_a=4.386$  nm) obtained at the assisting ion beam energy 300 eV. The MgO thin film surface feature is affected by the assisting ion beam energy.

Z. N. Yu *et al* reported the correlations between the discharge voltage and the surface roughness of the MgO thin film.[10] From Fig. 2 and Fig. 6, we observed the similar correlation between the firing voltage (or secondary electron emission coefficient,  $\gamma$ ) and the surface roughness. For the deposited MgO thin film with 300 eV assisting ion beam energy, it has the largest surface RMS roughness, the minimum firing voltage and the maximum secondary electron emission coefficient.

#### 4. Summary

In this paper, the MgO thin films were deposited with the oxygen ion beam assisted deposition method. The experimental results suggest that the assisting oxygen ion beam energy has direct effects on the structural and the discharging characteristics of MgO thin films. And the lowest firing inception voltage, the highest brightness, and the highest luminous efficiency were obtained when the assisting ion beam energy was 300 eV. Comparing with the No IBAD, it is considered that the ion beam assisted deposition method is suitable to the MgO thin films deposition with proper assisting ion beam energy.

#### 5. References

1. H. Bechtel, P. J. Heijnen, A. H. M. Holtslag, M Klein, R. Snikers, and H. Tolner, *IDW'98*, p527 (1998).
2. K. Amemiya, T. Komaki, and T. Nishio, *IDW'98*, p531 (1998).
3. J. H. Cho, R. H. Kim, K. W. Lee, G. Y. Yeom, H. J. Kim, J. K. Kim, and J. W. Park, *J. Materials Sci.*,

**350**, 173 (1999).

4. K. Oumi, H. Maotsumoto, K, Kashiwagi, and Y. Murayama, *Surf. And Coatings Tech.*, **169-170**, 562 (2003).
5. J. K. Kim, E. S. Lee, D. H. Kin, and D. G. Kim, *Thin Solid Films*, **447-448**, 95 (2004).
6. N. Yasui, H. Nomura, and A. I. Eetessabi, *Thin Solid Films*, **447-448**, 377 (2004).
7. Z. N. Yu, J. W. Seo, D. X. Zheng, and J. Sun, *Surf. And Coatings Tech.*, **163-164**, 398 (2003).
8. Y. Motoyama, Y. Hirano, Y. Ishii, Y. Murakami, and F. Sato, *J. Appl. Phys.*, **95**, 8419 (2004).
9. M. S. Park, D. H. Park, B. H. Kim, B. G. Ryu, and S. T. Kim, *SID Technical Digest*, p1399 (2006).
10. Eetessabi, H. Nomura, and Y. Tsukuda, *Thin Solid Films*, **447-448**, 383 (2004).